SP Science Press

ARTICLE

Preparation of Core-Shell Nanoparticles and Their Application in Precision Machining

Wang Youliang[1], Kang Yating[1], Zhang Wenjuan[2], Jiang Zhe[1], Yin Xincheng[1]

[1] School of Mechanical and Electrical Engineering, Lanzhou University of Technology, Lanzhou 730050, China; [2] State Key Laboratory of Advanced Processing and Recycling of Nonferrous Metals, Lanzhou University of Technology, Lanzhou 730050, China

Abstract: Preparation method of magnetic nanoparticles with core-shell structure was introduced, especially focusing on the preparation principle of sol-gel method, microemulsion method, and self-assembly technique. The application of core-shell nanoparticles in precision machining was discussed. The $Fe_3O_4@SiO_2$ composite particles were prepared by sol-gel method and were applied to the magnetorheological polishing of titanium alloy plates. Results show that core-shell nanoparticles with higher surface quality can be obtained after processing, compared with those after conventional abrasives. After polishing for 20 min, the surface roughness of the workpiece reaches 23 nm and the scratches are effectively reduced. Finally, the preparation and application of core-shell nanoparticles are summarized and prospected to provide a reference for further research on core-shell nanoparticles.

Key words: core-shell structure; magnetic composite nanoparticles; preparation; precision machining; applications

---

Nanocomposites are formed by combining two or more different materials, at least one of which has nanoscale dimensions. They have a variety of assembly forms, such as magnetic multilayer film systems[1], composite systems composed of magnetic nanoparticles embedded in thin films or other matrices (carbon tubes, graphene, etc)[2–4], and core-shell magnetic nanoparticles systems[5]. In core-shell nanomaterial systems, the inner core is mainly made of nanoparticles with strongly magnetism, such as 3d transition metals (Fe, Co, Ni), alloys (FeNi, FeCo, NiCo, Fe_3C, Fe_5C_2), oxides (Fe_3O_4, γ-Fe_2O_3), permanent magnetic ferrite-oxygen metals ($SrFe_{12}O_{19}$, $BaFe_{12}O_{19}$, etc). Meanwhile, the shell layer is mainly composed of non-magnetic or weakly magnetic materials such as insulators (SiO_2, Al_2O_3), semiconductors (ZnO, SnO_2), organic molecules (citric acid, oleic acid, polymers), carbon materials (carbon nanotubes, carbon nanorods, carbon nanobelts, carbon nanosheets, carbon nanorods, etc), and antiferromagnetic (CoO, NiO, $SrMoO_4$)[6].

Fe_3O_4 nanoparticles have shown great potential in controlling drug transport[7–9], imaging living organisms[10], labeling cells[11], developing biosensors[12], regenerative medicine[13], and treating wastewater[14–16] due to the excellent magnetic properties and biocompatibility[17]. However, Fe_3O_4 nanoparticles are prone to agglomeration due to the size effect, which constrains their clinical applications[18]. Nevertheless, Fe_3O_4 nanoparticles encapsulated by SiO_2 can overcome the above weakness in water. Therefore, $Fe_3O_4@SiO_2$ composite nanoparticles contribute to the further expansion of the application of Fe_3O_4 nanoparticles[19–20].

The preparation process of $Fe_3O_4@SiO_2$ nanoparticles is shown in Fig.1. Amino groups were firstly used to functionalize $Fe_3O_4@SiO_2$ nanoparticles through 3-aminopropyltriethoxysilane (APTES). The modified nanoparticles $Fe_3O_4@SiO_2$-NH_2 were functionalized with carboxyl functional groups by ethylenediaminetetraacetic acid (EDTA) through the formation of amide bonds. In addition, APTES was used to react in ethanol aqueous solution, and the layer of Ag nanoparticles was coated on its surface to modify the shell (TiO_2/Ag). Finally, $Fe_3O_4@SiO_2@TiO_2$/Ag complex photocatalytic materials with double shell structure were obtained. Oleic acid was modified onto the surface of Fe_3O_4 particles and then coated with cetyltrimethylammonium chloride

---

Fig.1 Schematic diagram of preparation and functionalization of $Fe_3O_4@SiO_2$ magnetic nanoparticles[21]

Fig.2 Schematic diagram of $Fe_3O_4@SiO_2$ composite nanoparticles prepared by Stöber method[24]

(CTAC) by hydrophobic action to obtain $Fe_3O_4@CTAC$ particles. The obtained composite particles have good antimicrobial properties. With Fe_3O_4 as the core, $Fe_3O_4@C$, $Fe_3O_4@CeO_2$, $Fe_3O_4@NiO$, and other core-shell materials can be obtained by surfactants. This encapsulation enables Fe_3O_4 nanoparticles to be more effectively utilized in various fields.

There are essentially two methods to coat Fe_3O_4 nanoparticles with SiO_2. The first method involves that the silicate is hydrolyzed in acidic conditions, whereas the second method involves the hydrolysis of ethyl orthosilicate in alkaline conditions. The second method can be further divided into the sol-gel method and the reversed-phase microemulsion method. The sol-gel method achieves the hydrolysis of ethyl orthosilicate in the ethanol/water system. In the reversed-phase microemulsion method, the hydrolysis of ethyl orthosilicate occurs at the interface between the water nanocore and the oil phase in the microemulsion. The sol-gel method and the reversed-phase microemulsion method are the common methods for the preparation of $Fe_3O_4@SiO_2$ core-shell nanoparticles[22].

In this research, the methods, principles, and mechanisms for core-shell nanoparticle preparation were introduced. Then, the application of core-shell nanoparticles in precision machining was introduced. The $Fe_3O_4@SiO_2$ composite particles were prepared and applied to magnetorheological polishing of titanium alloy plates. The preparation and application of core-shell nanoparticles were summarized and prospected.

1 Preparation Methods of Core-Shell Nanoparticles

1.1 Sol-gel method

In 1968, Stöber obtained SiO_2-coated magnetic nanoparticles by sol-gel method for the first time. Therefore, this method is also known as the Stöber method. The prepared process diagram of $Fe_3O_4@SiO_2$ composite nanoparticles is shown in Fig.2. The sol-gel method is usually conducted in an ethanol/water system because tetraethyl orthosilicate (TEOS) is insoluble in water but soluble in ethanol, which makes the hydrolysis reactions difficult to proceed. Hence, the ethanol is chosen as the cosolvent for TEOS and water to facilitate the mixing, and then the reaction is catalyzed by the alkaline substance that converts TEOS to silica[23].
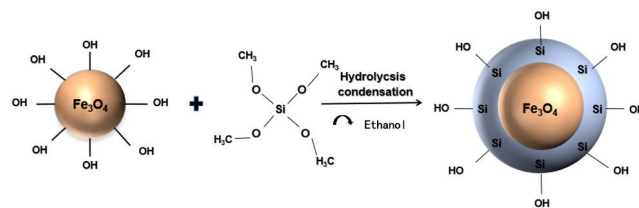
Silane coupling agents are commonly used as interfacial

modifiers to enhance adhesion and compatibility between core and shell materials when sol-gel methods are used. Silane coupling agents can react with the surface of material to form chemical or physical bonds, which enhance bonding between the core and shell materials. Organic silane is widely studied and used as coupling agent[20]. During the encapsulation process, $-Si-O-CH_3$ or $-Si-O-CH_2CH_3$ undergoes the hydrolysis reaction, as shown in Eq. (1), to produce the silanol group $-Si-OH$ firstly.

$$-Si-O-CH_2CH_3+H_2O \rightarrow -Si-OH+HO-CH_2CH_3 \tag{1}$$
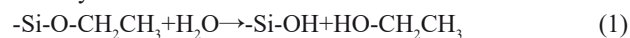
Under specific conditions, the hydroxyl group formed after the hydrolysis of silane undergoes the condensation reaction. The condensation reaction involves interactions between silanol and silanol hydroxyl groups, as well as with hydroxyl groups on the surface of the adjacent substance, leading to the formation of dense silicon layer. The silicon layer provides wrapping and protection to the core, while the hydroxyl group on the surface is linked with the hydroxyl group on the outer coating surface of X as shown in Eq.(2–3)[25]:

$$-Si-OH+-Si-OH \rightarrow -Si-O-Si-+H_2O \tag{2}$$

$$-Si-OH+-X-OH \rightarrow -Si-O-X-+H_2O \tag{3}$$
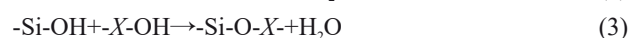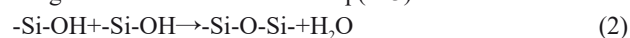
The main reactions in the process are the hydrolysis and condensation of TEOS. Meanwhile, some condensation reactions occur to produce the alcohol. The stability, dispersibility, and particle size of the product can be controlled by the TEOS amount[26–29], catalysts[28], reaction time[28], temperature[30], heating rate[31], and the parameters of stirring[32–33].

The presence of ammonia liquor in the ethanol-water system creates the alkaline environment, and the hydrolysis-condensation rate of TEOS is directly affected by ammonia liquor. When the ethanol/water ratio is low, the particles are easily dispersed. Conversely, the TEOS will hydrolyze rapidly again, leading to independent growth of SiO_2. The excess of ammonia liquor in the system causes SiO_2 to nucleate and grow. The increase in the amount of TEOS leads to the increase in thickness of SiO_2 shell and the more uniform particle size. The thickness of the SiO_2 shell can be controlled between $2 – 100$ nm by adjusting the amount of TEOS in isopropyl ethanol/water solution[34].

Different catalysts have been employed by Zou[28] to prepare $Fe_3O_4@SiO_2$ core-shell nanoparticles. The results show that NaOH and ammonia have better effects than triethylamine (TEA) catalysts. The effect of duration on coating and the film thickness was also analyzed. The coating process was implemented for 15 min to 20 h.

Guo et al[30] prepared $Fe_3O_4@SiO_2$ composite nanoparticles with the particle size distribution of 15–20 nm by controlling the temperature during the reaction. Sajid et al[31] prepared colloidal Fe_3O_4 nanoparticles with different particle sizes (15–20 nm) by controlling the heating rate and then achieved SiO_2 shell encapsulation to form $Fe_3O_4@SiO_2$ core-shell structure.

Chekalil et al[32] synthesized $Fe_3O_4@SiO_2$ composite nano-particles with excellent magnetic properties. However, due to the longer time of magnetic stirring during the process, the prepared composite nanoparticles were magnetized, leading to limited dispersion and easy agglomeration. This phenomenon can be effectively avoided by mechanical stirring[33].

The functionalization[35], magnetism[35], optical properties[36], and dielectric properties[37–38] of the core-shell structure particles were also studied. Meng[35] synthesized Fe_3O_4 magnetic nanoparticles and then coated them with SiO_2 by the sol-gel method. Subsequently, a series of sequential steps were conducted for surface modification, resulting in the preparation of carboxylation-modified $Fe_3O_4@SiO_2$ magnetic nanoparticles.

To characterize the magnetic properties of the $Fe_3O_4@SiO_2$ nanoparticles, the hysteresis lines of $Fe_3O_4@SiO_2$ nano-particles were measured at room temperature. As shown in Fig. 3, the magnetic properties of $Fe_3O_4@SiO_2$ nanoparticles obtained by sol-gel method were characterized and compared with those of pure Fe_3O_4 nanoparticles. The magnetization of nanoparticles increases gradually with the increase in the external magnetic field intensity, and finally tends to be stable. The coercivity and residual magnetization are close to zero, indicating that the Fe_3O_4 nanoparticles and $Fe_3O_4@SiO_2$ composite nanoparticles show excellent superparamag-netism[39]. The magnetization of the composite nanoparticles is notably reduced compared with that of Fe_3O_4 nanoparticles, which is attributed to the decreased mass fraction of Fe_3O_4 in the composite particles.

Khalid[36] and Divya[37] et al synthesized Fe_3O_4 and $Fe_3O_4@SiO_2$ composite nanoparticles. The synthesized $Fe_3O_4@SiO_2$ core-shell nanomaterials with enhanced optical parameters are considered as the suitable candidate in non-linear optical applications. Sakthisabarimoorthi et al[38] synthe-sized α-$Fe_2O_3@SiO_2$ core-shell nanospheres and studied their

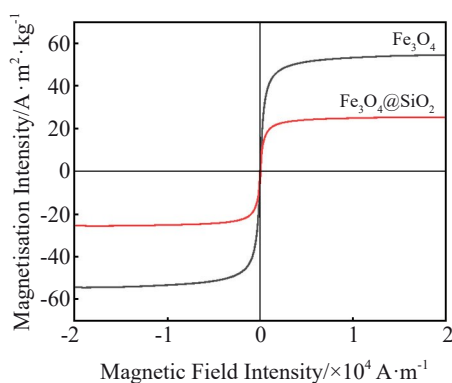dielectric behavior. Zhang et al[40] investigated the effect of shell thickness on absorption properties of $Co_3Fe_7@ZnO$, and explained the mechanism of microwave absorption. These studies have established the foundation for broadening the application of the core-shell structure.

The sol-gel method can be used to control the core-shell structure and fabricate mesoporous composite particles, ex-panding the applications of core-shell structures across var-ious fields. Fig.4 shows the schematic diagram of the synthesis of mesoporous nanoparticles using template agents. Zhao et al[41] employed the hydrolysis-condensation reaction to obtain mesoporous SiO_2/Fe_3O_4 nanospheres. Meanwhile, Sen et al[42] introduced the template agent hexadecyltrimethyl ammonium bromide (CTAB) and TEOS into the Fe_3O_4 suspension, and later removed the shell template CTAB through solvent extraction, resulting in mesoporous Fe_3O_4 nanoparticles, which were successfully used in magnetic bioseparation. Zhang et al[43] prepared mesoporous $Fe_3O_4@SiO_2$ composite material and used the composite material for the immobiliza-tion of laccase, proving that the composite material can be used as the excellent immobilization carrier after heat treatment. Recently, mesoporous $Fe_3O_4@SiO_2$ nanoparticles has been widely utilized in drug targeting, catalysis, and adsorption.

1.2 Reverse-phase microemulsion method

Reversed-phase microemulsions have been widely used for the preparation of nanoparticles with core-shell structure, because the microemulsions can provide the favorable reaction environment. The microemulsion has good stability and can be stored for long time without phase separation or precipitation. In addition, the microemulsion also has good controllability and adjustability. The procedure of the reversed-phase microemulsion method mainly includes the following steps: (1) obtaining the stable microemulsion system by adjusting the content of each component; (2) preparing nanoparticles with core-shell structure by reactions between the added new components and the original microemulsion.

The formation of SiO_2 involves the competitive process of TEOS hydrolysis, condensation, nucleation, and growth. Firstly, TEOS undergoes hydrolysis at the oil-water interface catalyzed in alkali conditions, as indicted in Eq.(4). Following the hydrolysis reaction, the condensation reactions depicted in Eq. (5) and Eq. (6) occur. The hydroxyl groups produced by hydrolysis are hydrophilic. When a sufficient number of hydrophilic groups are present, the hydrolysis products can penetrate the interfacial membrane and enter the aqueous phase. Once the hydrolysate enters the aqueous phase, the hydrolysis-condensation reaction occurs within the aqueous phase or at the interface. The composite particles are successfully formed through the heterogeneous growth of
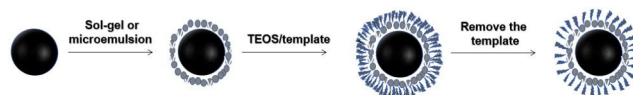

Fig.3 Hysteresis lines of Fe_3O_4 and $Fe_3O_4@SiO_2$ particles at room temperature

Fig.4 Schematic diagram of synthesis of mesoporous SiO_2 nano-particles using template agents[18]

SiO$_2$ particles formed by condensation reaction and collision on the surfaces of Fe$_3$O$_4$ nanoparticles.

$$\text{Si-OR+HOH} \rightarrow \text{Si-OH+R-OH} \tag{4}$$

$$\text{Si-OH+Si-OH} \rightarrow \text{Si-O-Si+HOH} \tag{5}$$

$$\text{Si-OH+Si-OR} \rightarrow \text{Si-O-Si+R-OH} \tag{6}$$

The effects of different stirring methods[44–46], one-step or two-step methods[46], surfactant[47], and TEOS dosage[45,48] on the products were also discussed. Fig. 5 shows images observed by transmission electron microscope (TEM) of core-shell nanoparticles prepared by different methods. It can be seen that the morphologies and dispersion of core-shell nanoparticles obtained by mechanical stirring are significantly better than those obtained by magnetic stirring and ultrasonic dispersion. Mechanical stirring can avoid magnetic attraction and have the high stirring speed, so it is easy to form core-shell composite nanoparticles with good dispersion and spherical morphology. The dispersion of nanoparticles using ultrasonic dispersion is better than that using magnetic stirring, thus significantly reducing adhesion between the dispersed nanoparticles. This improvement can be attributed to the fact that the ultrasonic process in the liquid medium accelerates the collision and reaction of SiO$_2$ particles on the surface of Fe$_3$O$_4$ magnetic particles, leading to the effective reduction in the agglomeration phenomenon of the particles.

In the process of one-step preparation, the structure and performance of the core-shell nanoparticles can be controlled by optimizing the experimental conditions according to the reaction conditions requirements. However, the control of the material structure is restricted due to the unique reaction condition. Meanwhile, the core-shell structure with excellent morphology can be obtained using the two-step method, which has the advantage that the reaction conditions can be optimized according to the core-shell material.

In addition, the stability of microemulsion is also influenced by the quantity of surfactant. The more stable microemulsion and more uniform core-shell structure can be achieved by increasing the amount of surfactant. The size and morphology of the particle can be easily controlled because the surfactant reduces the surface tension and facilitates the dispersion of the droplet. As the amount of surfactant increases, the thickness of shell materials is also increased, which is attributed to the increase in adsorption and deposition.

Moreover, when the TEOS content is too high, the surface potential of the particles is decreased, and the ionic strength of the solution is increased, which leads to the agglomeration and destabilization of Fe$_3$O$_4$ particles before encapsulation. As a result, a few Fe$_3$O$_4$ particles encapsulated by SiO$_2$ particles were observed. With the decrease in TEOS content, the dispersion of composite particles is improved. In addition, the particle sizes become more uniform.

The reversed-phase emulsion method has been used to prepare mesoporous composite nanoparticles with excellent magnetic properties[49–51]. These nanoparticles feature mesoporous core-shell structure, offering benefits, such as the large specific surface area, segregation effect, multifunctionality, and controllable structural stability. Mesoporous core-shell structured particles are widely used in drug delivery, catalysis, adsorption materials, and energy storage, due to their numerous advantages.

1.3 Self-assembly technique

Self-assembly technique relies on electrostatic interactions between molecules and the substrate or chemical bonding, in which particles with opposite charges are sequentially adsorbed layer-by-layer onto the substrate surface. The orderly molecular assembly system is formed through the spontaneous assembly of the core particles. Self-assembly technique enables precise tuning of shell composition and thickness at the supramolecular level.

Caruntu[52] and Qian[53] et al obtained Au/Fe$_3$O$_4$ nanoparticles and C/TiO$_2$ core-shell composite particles, respectively, using the electrostatic self-assembly technique. Wang et al[54] used the surface of core-shell microspheres with positive charge to effectively interact with the fluorescent shells of CdTe, resulting in the production of a novel multifunctional nano-complex particle. The prepared particles exhibit high sensitivity and can be used as a sensor for detecting Cu^{2+}. The obtained multifunctional nano-complex exhibits both magnetic and fluorescent effects. Furthermore, the multifunctional nano-complex possesses superparamag-
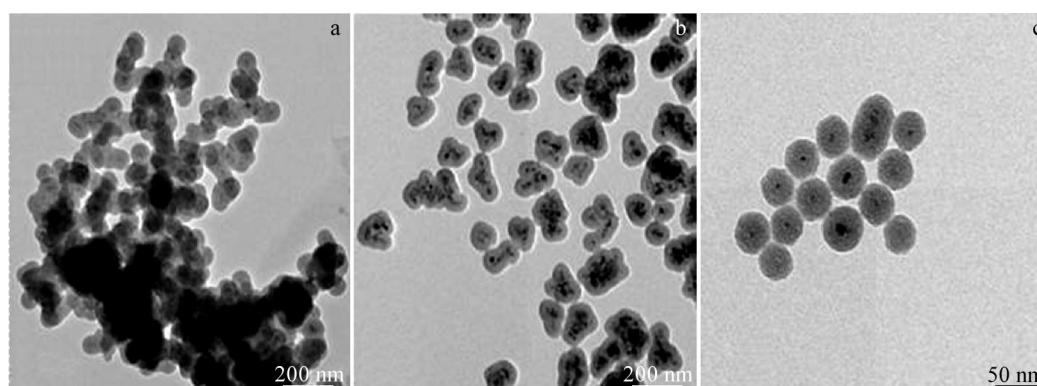

Fig.5 TEM images of core-shell nanoparticles obtained by different stirring dispersion methods: (a) magnetic stirring; (b) ultrasonic dispersion; (c) mechanical stirring[45]

netic properties and can be easily recovered using magnet. The fluorescent magnetic composite nanoparticles were prepared using the intermolecular electrostatic interactions[55–56]. Magnetic fluorescent polymer microcapsules were obtained by melamine formaldehyde as a template. Polyethylene naphthalate (PEn): sodium polystyrene sulfonate (PSS)/polyallylamine hydrochloride (PAH) with different electrical properties are alternately adsorbed on its surface, as shown in Fig. 6. Subsequently, the template is removed with hydrochloric acid, and Fe_3O_4 and CdTe particles with negative charge are infiltrated into the cavity.

(CdSe/ZnS)Fe_2O_3 composite nanoparticles with a particle size of 30 nm were synthesized by covalent bonding of thiols of organic sulfides with metals (Au and Ag) and semiconductors (CdSe and InP)[57]. Fe_3O_4/$NaYF_4$/SiO_2 bifunctional core-shell nanocomposites were created by self-assembly method[58]. These nanocomposites exhibit superparamagnetic properties and strong near-infrared luminescence.

Improved integration properties of multiple components can be achieved by self-assembly method through device at nanoscale. Therefore, controllable size and uniform morphology can be formed, in comparison to those obtained by single nano-assembly[59–60].

Star-shaped and linear block copolymer nano-self-assemblies were prepared by Zhang et al[61] using solution self-assembly method. They confirmed that the order of the blocks significantly affects the structure of the finally synthesized nano-self-assemblies. A theoretical basis for the construction of highly ordered nano-block polymer self-assembly is provided.

When different kinds of nanostructured units are assembled in different modes of action, the resulting assemblies not only possess the properties of the original nanostructured units, but also exhibit excellent aggregation properties in other aspects, such as optics[62–64], electricity[65–66], and magnetism[67–68]. These assemblies have significant application value in various fields, such as life sciences, medicine, industrial catalysts, and new energy sources.

2 Core-Shell Structured Particles for Precision Machining Application

With the development of industry, the characteristics of non-ferrous metal alloys are becoming more and more prominent, and they are widely used in many industries such as aerospace, shipbuilding, and electronics[69]. Due to the low hardness of most non-ferrous metals, the surface grinding of t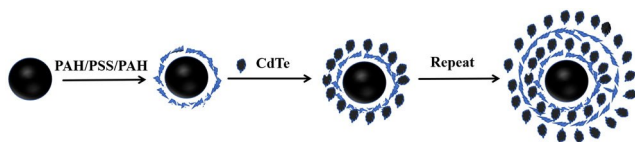his soft metal material is the major problem in the grinding process. Magnetic nanoparticles with core-shell structures also have advantages in precision machining compared with traditional abrasives. By regulating the composition, structure, and properties of the nanoparticles with core-shell structures, nanocomposite particles with various functions are prepared, which are expected to improve the quality of precision machining of traditional abrasive grains.

Yano et al[70] prepared the polishing liquid, which was composed of alumina/organic resin with core-shell structure, and conducted chemical mechanical polishing (CMP) tests on low K (dielectric constant) materials, such as aluminum. The 2-step CMP was employed. The first step of the process is to remove aluminum and stop polishing on the niobium liner, and the removal of the niobium liner is the second step. In the initial CMP step, the slurry includes resin particles (200 nm) and primary alumina particles (20 nm). The polishing pad was IC-1000/SUBA-400. For the subsequent CMP step, the silica/resin composite abrasive was used with the Politex pad. Experiments on the EBARA EPO-222 machine involved the use of slurry containing the mixture of alumina and resin, resulting in the polishing rate 10 times faster than that achieved with alumina slurry alone. Results of the experiments confirm that the grinding wheel produces fewer scratches, resulting in the smoother surface after polishing. Furthermore, the application of the polishing fluid significantly enhances the efficiency of the polishing process. Experiments have proved that the grinding wheel has fewer scratches, the surface is flatter after being processed by polishing fluid, and the polishing efficiency is greatly improved.

In Ref. [71], PS/CeO_2 abrasive with spherical core-shell structure was used for polishing experiments. Silicon thermal oxides were polished with the carrier disk pressure of 24.8 kPa, polishing slurry pH of 10, slurry flow rate of 150 mL/min, platen speed of 90 r/min, and temperature of 20 °C. The results reveal that the polishing quality can be effectively enhanced by the composite abrasives while ensuring the consistent material removal rate. The surface quality of oxide CMP can be significantly improved by the organic/inorganic composite abrasive. The composite abrasive has the potential application prospect in the CMP of copper and low dielectric constant (low K) material.

In Ref. [72], the composite abrasive particles consisted of solid silica (sSiO_2) core and mesoporous silica (mSiO_2) shell for the polishing of SiO_2 films. Polishing experiments were conducted using TegraForce-1/TrgraPol-15 polishing machine (Struers, Denmark). The polishing conditions included the down pressure of $2.76×10^4$ Pa, the carrier/platen speed of 120/90 r/min, the slurry flow rate of 200 mL/min, and polishing time of 1 min. As a result, the removal rate of composite particles is much higher because the composite material has elastic deformation, which increases the contact area between the abrasive material and the substrate. This is because the surface hardness and elasticity modulus of composite particles are much lower than those of SiO_2 particles, leading to the reduction of the contact stress.

A new type of SiO_2/CeO_2 composite abrasive particle

Fig.6 Schematic diagram of fluorescent core-shell structured composite nanoparticles prepared by self-assembly method[8]

with core-shell structure was prepared by Xiao et al[73] using $CO(NH_2)_2$, $(NH_4)_2Ce(NO_3)_6$, and SiO_2 as the main materials. The composite abrasive particles were then formulated into slurry, which was used for grinding experiments on the glass substrate of the digital optical disc. The polishing test used the SPEEDFAM-16B4M polishing machine from the Japanese company SPEEDFAM. The test parameters included the polishing pressure of 0.39 MPa, lower disk speed of 9 r/min, and polishing liquid flow rate of 800 mL/min. DPC5150 polishing pad produced by RODEL company was selected. After grinding for 1 h, it is observed that the ripple on the surface of the glass substrate is significantly reduced, resulting in the smoother surface and obvious improvement in surface quality.

Alumina/carbon composite abrasive particles were synthesized by Yan et al[74], and they were applied to the surface processing of monocrystalline silicon. The aqueous polishing solution for core-shell nanodiamond/carbon composites was formulated at the concentration of 1wt% and the pH value of 10. The polishing time in the experiment was 1 h, the polishing speed was 280 r/min, and the polishing pressure was 10 N. The results show that the polishing solution can effectively reduce surface scratches, but the material removal rate is not high compared with that of the nanodiamond water-based polishing solution.

SiO_2 was coated on carbonyl iron (CI) particles by Pan et al[75] to create the magnetorheological fluid that was used for polishing sapphire. Ultrasonic-assisted magnetorheological polishing (UAMP) of sapphire using $Fe_3O_4@SiO_2$ nanocomposite particles with core-shell structure was studied by Zhai et al[76]. The schematic diagram of polishing principle is shown in Fig. 7. The high-intensity magnetic field area is generated by the permanent magnet, where the core-shell abrasive particles are aligned along the magnetic field lines to form the chain-like structure. Material removal is achieved through the interaction between the sapphire surface and the abrasive particles. The polishing pressure of sapphire wafer is 25 kPa, the polishing time is 2 h, the ultrasonic amplitude is 50 μm, and the ultrasonic frequency is 20 kHz. The contact model between abrasives and workpieces is depicted in Fig. 8. When core-shell abrasive particles are in contact with the sapphire under the action of force, the abrasives become ellipsoid shape, and the actual contact area expands to the larger circle,
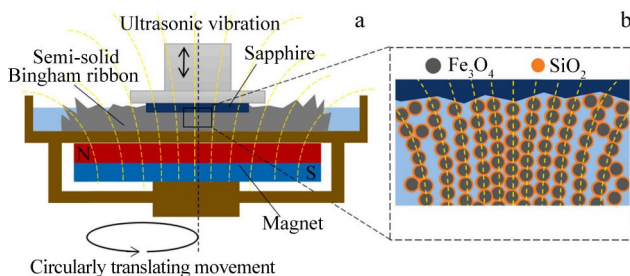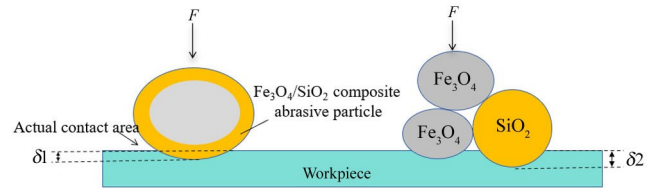
Fig.8 Schematic diagrams of $Fe_3O_4@SiO_2$ core-shell abrasive (a) and mixed abrasive contact model with workpiece[76]

which improves the material removal rate. The largest sapphire material removal rate of 1.974 μm/h and comparatively low surface roughness R_a of 0.442 nm were achieved by UAMP for Fe_3O_4/SiO_2 core-shell abrasive particles. It is observed that $Fe_3O_4@SiO_2$ core-shell abrasive particles exhibit excellent polishing properties. A smooth and defect-free machined surface can be achieved.

3 Experiment Results

In order to verify the feasibility of core-shell abrasive particles for precision machining, relevant experiments were conducted. Firstly, $Fe_3O_4@SiO_2$ composite nanoparticles were prepared by sol-gel method and formulated as water-based polishing solution. The magnetorheological polishing technique was used to polish the titanium alloy plate, and the experimental conditions are shown in Table 1. The composition ratios of polishing liquid were carbonyl iron powder of 20wt%, cellulose of 2wt%, abrasive particle of 20wt%, and water-based magnetic fluid of 58wt%.

After polishing for 20 min, the surface morphology of the workpiece was measured using the white light interferometer. The three-dimensional (3D) topography and corresponding S_a values of the workpiece before and after polishing with different abrasive particles are shown in Fig.9.

From the 3D morphologies of the workpiece surface in Fig.9a, it can be seen that there are pits and irregular scratches on the initial surface of the workpiece. Compared with the use of mixed Fe_3O_4-SiO_2 abrasives, the surface of workpieces polished with core-shell abrasives is much flatter with the surface roughness S_a of 23 nm. As shown in Fig. 9b, the original defects on the surface of the workpiece are removed. As shown in Fig.9c, the surface roughness of the workpiece is

Fig.7 Schematic diagrams of principle of UAMP (a) and composite abrasive/wafer contact model (b)[73]

Table1 Experimental parameters of magnetorheological polishing technique

Parameter	Value
Workpieces	TC4 plate, 50 mm×50 mm×1 mm
Permanent magnet (N52)	B=0.56 T, Φ10 mm×10 mm
Eccentricity, r/mm	1
Workpiece rotational speed, n_w/r·min^{-1}	500
Magnet rotational speed, n_c/r·min^{-1}	600
Working gap, Δ/mm	1
Polishing time, t/min	20

S_a: 0.203 μm
S_q: 0.271 μm
S_z: 3.859 μm

S_a: 0.023 μm
S_q: 0.031 μm
S_z: 1.428 μm

S_a: 0.052 μm
S_q: 0.085 μm
S_z: 2.301 μm
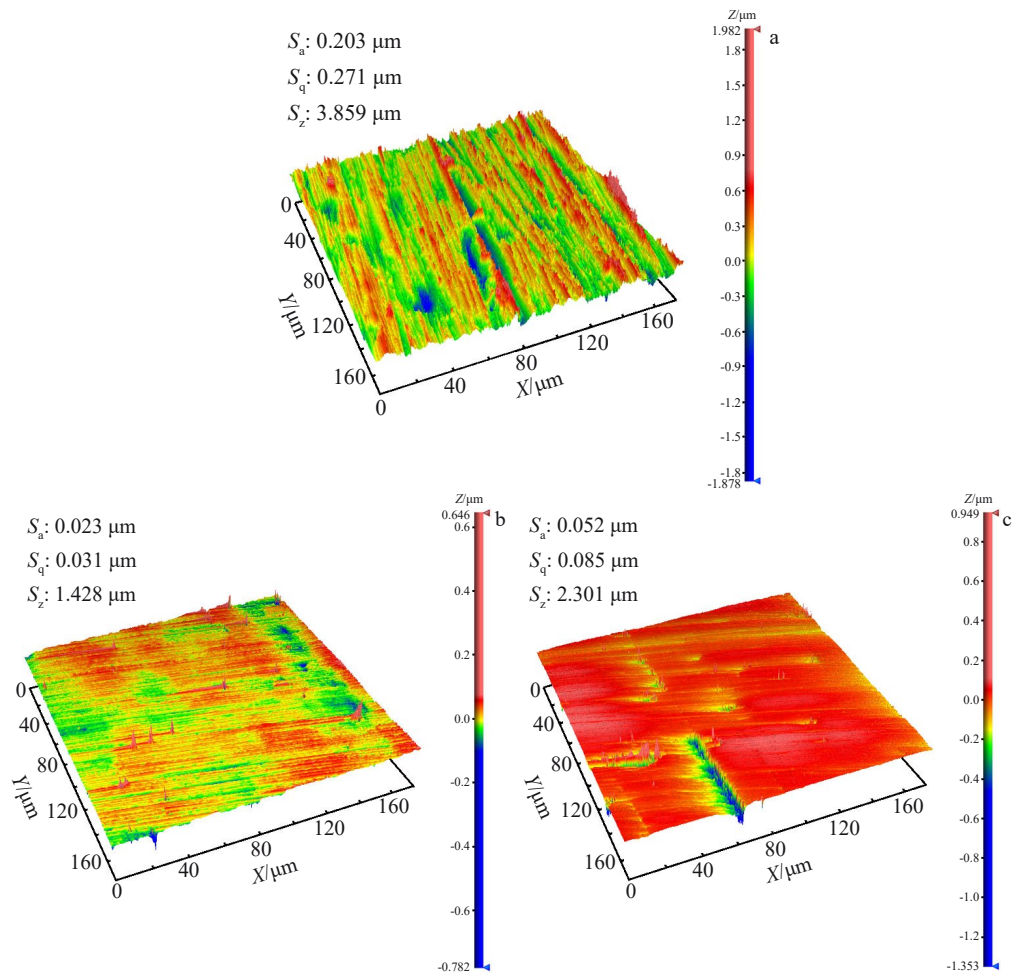
Fig.9　3D morphologies of workpiece surface before polishing (a) and polished by Fe_3O_4@SiO_2 core-shell abrasives (b) and mixed Fe_3O_4-SiO_2 abrasives (c)

reduced, but the original defects are not completely removed.

It has been demonstrated that the surface scratches of the workpiece can be effectively reduced by nanoparticles with core-shell structure. Furthermore, the relatively smooth surface can be obtained. The material removal rate is higher and the surface roughness is lower when the core-shell nanoparticles are used. At present, the application of core-shell nanoparticles are widely researched for the precision machining of semiconductor materials, brittle and hard materials, metal materials, etc. These findings indicate that

nanoparticles with core-shell structures have great application potential in precision machining.

The significance of applying core-shell structural particles to precision machining is substantial, as shown in Table 2. The composite particles combine the properties of the original particles. Fe_3O_4 coated with non-magnetic abrasive particles can effectively reduce agglomeration and improve processing efficiency. In addition, the shell material can be used to chemically react with the workpiece surface to improve the material removal rate, thereby improving the efficiency. In

Table 2　Summary and assessment of composite nanoparticles with core-shell structure in precision machining application

Processed material	Composite particle type	Processing method	Processing effect	Ref.
Al	Aluminum oxide/ organic particles		Reduced scratches and high material removal rate	[70]
Silicon wafer	PS/CeO_2 Al_2O_3/C	CMP	High surface quality, high material removal rate, reduced scratches, and low material removal rate	[71,74]
SiO_2 thin film	sSiO_2/mSiO_2		High material removal rate	[72]
Glass substrate	SiO_2/CeO_2		Reduced surface ripples	[73]
Sapphire	SiO_2/CI	Magnetorheological polishing	High polishing efficiency	[75]
	Fe_3O_4@SiO_2	UAMP	Obtained smooth and defect-free surfaces	[76]

addition, core-shell structure particles can also be used to process superhard materials. In the grinding and polishing process, high-hardness abrasive particles, such as diamond and alumina, directly impact the machined surface, and cause hard impact on the machined surface, resulting in large scratches, cracks, pits, and other microscopic defects. When the surface of the abrasive is coated with a layer of soft material, the scratches, cracks, pits, and other defects generated in the polishing process can be reduced, which is better than the results using the single abrasive.

4 Conclusions and Prospects

In recent years, more and more scholars have paid attention to core-shell nanocomposites. Core-shell nanocomposite can realize the composite and complementary of heterogeneous materials, and such material are more advantageous than single-component nanoparticles in terms of structure and performance. Therefore, compared with single-component nanoparticles, core-shell nanocomposites have the broader application prospect.

So far, a large number of research have been carried out on preparing magnetic composite nanoparticles with the core-shell structure. However, some of the detailed reaction mechanisms require further refinement and improvement. Currently, the synthesis of core-shell nanomaterials is hindered by limited theoretical foundation. A more comprehensive understanding of the physical and chemical phenomena involved in the reaction is necessary. In the future, more attention needs to be paid to mass production preparation. Because of the complexity of preparation process, the large-scale application of core-shell structure abrasive particles in industry has become a problem. The core-shell structure nanomaterials are easy to agglomerate in the preparation process, which should be paid attention.

With the deepening of future research, the preparation method of composite nanoparticles with core-shell structure is expected to become more convenient. Moreover, their application field will be more and more broad and close to the daily life. The continuous energy source for the development of nanotechnology will certainly be provided by the exploration and research on the application of core-shell composite nanoparticles.

Besides, self-assembly technique has been explored from different perspectives, such as Van der Waals force, static electricity, hydrogen bond, magnetism, and entropy effect. New development directions have been proposed on this basis. However, many problems persist in the self-assembly mechanism, precise control of structure, and large-scale preparation. Research on self-assembly technique mainly involves the synthesis and preparation of assemblies. Therefore, further study and discussion on the self-assembly mechanism are necessary. In terms of precise control of structure, the main research line of structure-property-application should be grasped to realize the orderly control of the microstructure of nano-assemblies at controllable macroscopic level. In terms of mass production, new materials with lower cost should be explored as substitutes for precious metals, semiconductors, and other materials to realize industrial production of nanoscale self-assembled materials[77].

References

1 Nogués J, Schuller I K. *Journal of Magnetism and Magnetic Materials*[J], 1999, 192(2): 203

2 Bianco L D, Fiorani D, Testa A M *et al. Physical Review B*[J], 2004, 70(5): 052401

3 Grzelczak M, Correa-Duarte M A, Salgueiriño-Maceira V *et al. Angewandte Chemie International Edition*[J], 2007, 46(37): 7026

4 Tian Z M, Yuan S L, Yin S Y *et al. Physical Review Letters*[J], 2008, 93: 222505

5 Liu W, Zhong W, Du Y W. *Journal of Nanoscience and Nanotechnology*[J], 2008, 8: 2781

6 He Xuemin, Zhong Wei, Du Youwei. *Acta Physica Sinica*[J], 2018, 67(22): 227501 (in Chinese)

7 Laurent S, Forge D, Port M *et al. Chemical Reviews*[J], 2008, 108(6): 2064

8 Xu D D, Xie R, Xu T Y *et al. RSC Advances*[J], 2016, 6(91): 88248

9 Chen W H, Luo G F, Lei Q *et al. Biomaterials*[J], 2016, 76: 87

10 Salgueiriño-Maceira V, Correa-Duarte M A. *Advanced Materials*[J], 2007, 19(23): 4131

11 Knopp D, Tang D, Niessner R. *Analytica Chimica Acta*[J], 2009, 647(1): 14

12 Schärtl W. *Nanoscale*[J], 2010, 2: 829

13 Stanciu L, Won Y H, Ganesana M *et al. Sensors*[J], 2009, 9(4): 2976

14 Zhang Qiang. *Photocatalytic Activity and Synthesis Technology of TiO₂-SiO₂-Fe₃O₄ Nanoparticles with Core-Shell Structure*[D]. Taiyuan: North University of China, 2013 (in Chinese)

15 Yuan J S, Zhang Y, Zhang X Y *et al. International Journal of Metallurgy and Materials*[J], 2022, 30(1): 165

16 Habila M A, Moshab M S, El-Toni A M *et al. ACS Omega*[J], 2023, 8(8): 7626

17 Sun Pengfei, Cao Xiangrong, Zhu Hao *et al. Chinese Journal of Tissue Engineering Research*[J], 2012, 16(3): 413 (in Chinese)

18 Liu Bing, Wang Deping, Yao Aihua *et al. Journal of the Chinese Ceramic Society*[J], 2008, 36(4): 569 (in Chinese)

19 Arruebo M, Galán M, Navascués N *et al. Chemistry of Materials*[J], 2006, 18(7): 1911

20 Liu X P, Ma Z Y, Xing J M *et al, Journal of Magnetism and Magnetic Materials*[J], 2004, 270(1–2): 1

21 Salman D, Juzsakova T, Al-Mayyahi M A *et al. Journal of Physics: Conference Series*[J], 2021, 1773: 012039

22 Huang Gengrui, Liang Zhiling, Luo Yiyuan *et al. Chemical Engineering & Equipment*[J], 2020, (2): 206 (in Chinese)

23 Shen Zhong. *Chemical Industry and Engineering Progress*[J], 1993(4): 52 (in Chinese)

24 Chae H S, Kim S D, Piao S H *et al. Colloid and Polymer Sci-

ence[J], 2016, 294: 647

25 Lai Li. *The Study on Functionalized Magnetic Core/Shell Structured $Fe_3O_4@SiO_2$ Nano-particles Adsorbents and Properties of Removing Contaminants from Water*[D]. Shanghai: Shanghai Jiao Tong University, 2020 (in Chinese)

26 Feng Yan. *Organic Silane Modification and Functionalization Research of Fe_3O_4 Nanoparticles*[D]. Harbin: Harbin Institute of Technology, 2006 (in Chinese)

27 Deng Y H, Wang C C, Hu J H *et al. Colloids and Surfaces A: Physicochemical and Engineering Aspects*[J], 2005, 262(1–3): 87

28 Zou J, Peng Y G, Tang Y Y. *RSC Advances*[J], 2014, 4(19): 9693

29 Zhang Le, Shao Huiping, Zheng Hang *et al. Rare Metal Materials and Engineering*[J], 2018, 47(2): 594 (in Chinese)

30 Guo Yan, Xiao Zundong. *Journal of Jilin Institute of Architecture & Civil Engineering*[J], 2011, 28(4): 78 (in Chinese)

31 Sajid M, Shuja S, Rong H P *et al. Progress in Natural Science: Materials International*[J], 2023, 33(1): 116

32 Chekalil N, Tarhini M, Elaissari A *et al. Research on Chemical Intermediates*[J], 2019, 45: 4847

33 Liao Peng, Li Na, Liu Jialiang *et al. Journal of Chengdu University of Technology* (*Science & Technology Edition*) [J], 2019, 46(1): 118 (in Chinese)

34 Lu Y, Yin Y, Mayers B T *et al. Nano Letters*[J], 2002, 2(3): 183

35 Meng Yan. *Applied Chemical Industry*[J], 2019, 48(9): 2134 (in Chinese)

36 Khalid A, Ahmed R M, Taha M *et al. Journal of Alloys and Compounds*[J], 2023, 947: 169639

37 Divya S, Lims S C, Manivannan M *et al. Journal of Alloys and Compounds*[J], 2022, 919: 165751

38 Sakthisabarimoorthi A, Martin B D S A, Jose M *et al. Journal of Alloys and Compounds*[J], 2019, 771: 1

39 Xue Hongta, Shen Shuifa, Pan Haibo *et al. Journal of Inorganic Materials*[J], 2009, 24(3): 577 (in Chinese)

40 Zhang Haoyan, Yang Jinnan, Zhang Kaigen *et al. The Chinese Journal of Nonferrous Metals*[J], 2023, 33(9): 2920 (in Chinese)

41 Zhao W R, Gu J L, Zhang L X *et al. Journal of the American Chemical Society*[J], 2005, 127(25): 8916

42 Sen T, Sebastianelli A, Bruce I J. *Journal of the American Chemical Society*[J], 2006, 128(22): 7130

43 Zhang Hang, Bi Hong, Xiao Yazhong. *China Sciencepaper*[J], 2009, 4(9): 650 (in Chinese)

44 Dong Jingwei, Zhang Zhirong, Zhang Yang *et al. Materials Reports*[J], 2010, 24(S1): 166 (in Chinese)

45 Zheng Haoran, Liu Gang, Wu Huixia *et al. Chemical Research and Application*[J], 2010, 22(5): 587 (in Chinese)

46 Min Jie, He Lihua, Zheng Rong *et al. Modern Chemical Industry*[J], 2021, 41(2): 146 (in Chinese)

47 Cho S J, Idrobo J C, Olamit J *et al. Chemistry of Materials*[J], 2005, 17(12): 3181

48 Santra S, Tapec R, Theodoropoulou N *et al. Langmuir*[J], 2001, 17(10): 2900

49 Yi D K, Lee S S, Georgia C *et al. Chemistry of Materials*[J], 2006, 18(3): 614

50 Kim J, Lee J E, Lee J *et al. Journal of the American Chemical Society*[J], 2006, 128: 688

51 Du Xueyan, Ma Fen, Li Fang *et al. Journal of Lanzhou University of Technology*[J], 2011, 37(2): 22 (in Chinese)

52 Caruntu D, Cushing B L, Caruntu G *et al. Chemistry of Materials*[J], 2005, 17(13): 3398

53 Qian H, Hu Y, Liu Y *et al. Materials Letters*[J], 2012, 68: 174

54 Wang H G, Sun L, Li Y P *et al. Langmuir the ACS Journal of Surfaces & Colloids*[J], 2011, 27(18): 11609

55 Hong X, Li J, Wang M *et al. Chemistry of Materials*[J], 2004, 16(21): 4022

56 Zebli B, Susha A S, Sukhorukov G B *et al. Langmuir*[J], 2005, 21(10): 4262

57 Wang D, He J, Rosenzweig N *et al. Nano Letters*[J], 2004, 4(3): 409

58 Zhang M, Shi S, Meng J *et al. Journal of Physical Chemistry C*[J], 2008, 112(8): 2825

59 Chen W, Bian A, Agarwal A *et al. Nano Letters*[J], 2009, 9(5): 2153

60 Luo D, Yan C, Wang T. *Small*[J], 2015, 11(45): 5984

61 Zhang Y, Guan T Y, Han G *et al. Macromolecules*[J], 2019, 52(2): 718

62 Jain P K, Eustis S, El-Sayed M A. *Journal of Physical Chemistry B*[J], 2006, 110(37): 18243

63 Talapin D V, Shevchenko E V, Murray C B *et al. Journal of the American Chemical Society*[J], 2004, 126(40): 12984

64 Wang M M, Zhang J, Wang P *et al. Nano Research*[J], 2018, 11(7): 3854

65 Brown P, Kamat P V. *Journal of the American Chemical Society*[J], 2008, 130(28): 889

66 Xing F K, Ren H Q, Ji C C *et al. Rare Metal Materials and Engineering*[J], 2017, 46(11): 3253

67 Li Cheng, Zhang Shaohua, Fu Gang *et al. Journal of Fujian Normal University* (*Natural Science Edition*)[J], 2023, 39(6): 76 (in Chinese)

68 Lu A H, Salabas E L, Schuth F. *Angewandte Chemie International Edition*[J], 2007, 46(8): 1222

69 Qing Weiwei, Wen Huaixing. *Mechanical Engineering & Automation*[J], 2017(6): 133 (in Chinese)

70 Yano H, Matsui Y, Minamihaba G *et al. MRS Online Proceedings Library*[J], 2001, 671(1): 24

71 Chen Yang, Long Renwei, Chen Zhigang *et al. Tribology*[J], 2010, 30(1): 9 (in Chinese)

72 Chen A, Yang C, Wang Y Y *et al. Journal of Alloys and Compounds*[J], 2016, 663: 60

73 Xiao Baoqi, Lei Hong. *Tribology*[J], 2008, 28(2): 103 (in Chinese)

74 Yan Shuang. *Research on Preparation and Properties of Core-Shell Composite Abrasives*[D]. Qinhuangdao: Yanshan Univer-

sity, 2019 (in Chinese)

75 Pan J S, Chen Z J, Yan Q S. *Smart Materials and Structures*[J], 2020, 29: 114003

76 Zhai Q, Zhai W J, Gao B *et al. Ceramics International*[J], 2021,

47(22): 31681

77 Wang Jun, Wang Tie. *Chemical Journal of Chinese Universities*[J], 2020, 41(3): 377 (in Chinese)

核壳结构粒子制备及在精密加工中的应用

王有良[1]，康娅婷[1]，张文娟[2]，姜　哲[1]，尹新城[1]

(1. 兰州理工大学 机电工程学院，甘肃 兰州 730050)
(2. 兰州理工大学 省部共建有色金属先进加工与再利用国家重点实验室，甘肃 兰州 730050)

摘　要： 研究了核壳结构磁性纳米粒子的制备方法，重点阐述了溶胶凝胶法、微乳液法、自组装技术的制备原理机制，探讨了近年来关于核壳结构在精密加工方面的相关研究进展。利用溶胶凝胶法制备了 $Fe_3O_4@SiO_2$ 复合粒子，并将其应用于钛合金板材的磁流变抛光中。结果表明，与传统磨粒相比，核壳结构磨粒加工后可获得更高的表面质量。经过 20 min 抛光后，工件面粗糙度达到了 23 nm，并且有效地减少了划痕。最后，对核壳结构纳米粒子的制备和应用进行了总结和展望，为核壳结构纳米粒子进一步研究提供参考。

关键词： 核壳结构；磁性复合纳米粒子；制备；精密加工；应用

作者简介：王有良，男，1986 年生，博士，副教授，兰州理工大学机电工程学院，甘肃 兰州 730050，E-mail: wangyouliang20@163.com